

Kondo Scaling in the Optical Response of $\text{YbIn}_{1-x}\text{Ag}_x\text{Cu}_4$

Jason N. Hancock, Tim McKnew, and Zack Schlesinger

Physics Department, University of California Santa Cruz, Santa Cruz, California 95064, USA

John L. Sarrao

Los Alamos National Laboratory, Mail Stop K764, Los Alamos, New Mexico 87545, USA

Zach Fisk

*National High Magnetic Field Laboratory, Tallahassee, Florida 32310, USA
and Department of Physics, Florida State University, Tallahassee, Florida 32306, USA
(Received 27 October 2003; published 6 May 2004)*

Theoretical work on Kondo systems predicts universality in the scaling of observable quantities with the Kondo temperature, T_K . Here we report infrared-frequency optical response measurements of the correlated system $\text{YbIn}_{1-x}\text{Ag}_x\text{Cu}_4$. We observe that x -dependent variations in the frequency and strength of a low-energy excitation are related to the x -dependent Kondo temperature. Comparison of the inferred trends with existing theory and a model calculation provides a framework in which to view these experimental results as scaling phenomena arising from local-moment/conduction electron hybridization.

DOI: 10.1103/PhysRevLett.92.186405

PACS numbers: 71.27.+a, 75.20.Hr, 75.30.Mb

The study of the Kondo problem has contributed much in the way of theoretical technology (e.g., renormalization group) as well as insight into the possible manifestations and phenomenologies of interacting systems with many degrees of freedom. One unifying effect born from the years of investigation is the Kondo resonance—a many-body collective excitation responsible for much of the interesting low-energy behavior displayed by rare-earth and transition metal systems.

YbAgCu_4 is a moderately heavy fermion system. At high temperature, the $j = \frac{7}{2}$ Yb moment acts independently of the carriers, while at low temperatures, screening of that moment leads to an enhanced Pauli paramagnetic susceptibility [1,2] and Sommerfeld coefficient ($\gamma \sim 250$ mJ/mol K²), reflecting a large effective carrier mass [2], or equivalently, a large density of states near the chemical potential. The crossover between the high and low temperature regimes occurs around a characteristic scale T_K , which is intimately related to the degree to which the low temperature properties are enhanced.

Substituting In for Ag gives very different behavior. YbInCu_4 displays a first-order isostructural electronic phase transition at $T_v \simeq 42$ K from a free-moment semimetal to a low-temperature metallic mixed-valent phase [3,4]. This phase transition begins a phase boundary in the $x - T$ plane of $\text{YbIn}_{1-x}\text{Ag}_x\text{Cu}_4$ which increases in temperature as x is increased and ends in a critical point around $x \simeq 0.3$. This phase boundary is of considerable interest [1–7] because it involves mainly electronic degrees of freedom and because there is as yet no real understanding of or agreement regarding its fundamental origin. When approaching an understanding, one must address the periodic Anderson model (PAM), which pro-

vides a powerful basis for interpreting the phenomenology of heavy fermion and mixed-valent systems, where crossover behavior is the norm. While much of the phenomenology of $\text{YbIn}_{1-x}\text{Ag}_x\text{Cu}_4$ is consistent with the PAM, the occurrence of an unexpected phase transition at low x could indicate the need for an additional interaction term in its minimal model Hamiltonian. It is natural in this context to consider whether adding conduction electron interactions (c.f. Giamarchi *et al.* [8] and Freericks *et al.* [7]) which are not generally included in the PAM, could provide competing influences necessary to understand the origin of this phase transition. Further exploration in this area may help establish a connection between the domain of Mott-Hubbard physics, where strong conduction electron interactions lead to a phase transition, and the moment-compensation physics of the Anderson and Kondo models.

In low-temperature YbInCu_4 , where the Kondo scale is large, there appears a distinct feature in the midinfrared conductivity that is not present in the high temperature phase [5]. It has been suggested that similar midinfrared features found in other heavy fermion materials [5,9,10] are a manifestation of local-moment phenomena [11–14]. Here, by studying the Ag concentration dependence of the dynamical conductivity in $\text{YbIn}_{1-x}\text{Ag}_x\text{Cu}_4$, we effectively vary T_K within the low-temperature phase and observe systematic changes in characteristics of the midinfrared excitation. We then explore the scaling behavior of this excitation in the context of a simple local-moment hybridization picture, and establish both the identification and phenomenology of the optical signature of the Kondo resonance.

We have measured the reflectivity of single crystals of a sequence of samples of $\text{YbIn}_{1-x}\text{Ag}_x\text{Cu}_4$ with

$x = 0, 0.3, 0.5, 0.75,$ and 1.0 . Our measurements cover the frequency range from 5 meV to 6.2 eV with detailed temperature dependent data taken between 5 and 2.8 eV. A Kramers-Kronig transform is applied to the measured reflectivity to determine the real and imaginary parts of the dynamical conductivity. For the purposes of the transform, Hagen-Rubens terminations are used below 5 meV. At high frequency (above 6 eV) each reflectivity spectrum is extrapolated to a common value of 0.08 at $\omega = 15$ eV and then continued as a constant to 25 eV. Between 25 and 50 eV an ω^{-2} form is used for $R(\omega)$ and above 50 eV the free-electron form ω^{-4} is assumed. In order to assure that our essential results below 1 eV do not depend on the high-frequency extrapolations, we have experimented with a number of termination protocols including other common values and coalescence frequencies as well as constant extrapolations above 6.2 eV. These show convincingly that our results regarding trends in the x and T_K dependence of $\sigma_1(\omega)$ below 1 eV are not significantly influenced by any of the extrapolations above 6.2 eV.

Figure 1 shows the low-temperature conductivity for the five x values studied. A prominent feature centered around $\frac{1}{4}$ eV for $x = 0$ (YbInCu₄) changes only slightly as x is increased to 0.3; however, further doping to $x = 0.5$ and 0.75 causes both a redshift and strengthening of this feature. Triangles mark the frequency of the peak of $\sigma_1(\omega)$ and vertical bars mark the location of a threshold frequency obtained from a model calculation described below.

In Fig. 2(a) these two characteristic frequencies, corresponding, respectively, to the peak and threshold of this excitation, are plotted both as a function of x and as a function of T_K . Values of T_K as a function of x are obtained from measurements of magnetic susceptibility [1]. The complex dependence on x becomes monotonic when plotted vs T_K . The dotted curves in Fig. 2(a) refer to a theoretical scaling described below.

In Fig. 2(b) an integral of $\sigma_1(\omega)$ in the vicinity of this excitation is shown as a function of x and T_K . This spectral weight, or strength, is defined by the integral,

$$n(\omega) = \frac{2m}{\pi e^2} \int_{0^+}^{\omega} \sigma_1(\omega') d\omega', \quad (1)$$

where the limits of integration, 6 meV and 0.5 eV, encompass the $\frac{1}{4}$ eV excitation and exclude a very small Drude peak at very low frequency. Neither integration limit is critical; in fact a lower limit of 0 and upper limits between anywhere between 0.4 and 1 eV produce the same x dependence which makes one confident that the n versus x dependence shown here is an essential characteristic of the data, and independent of any of the details of the choices we have made in the analysis.

Our discussion of the data centers on the PAM dispersion relations illustrated in the inset of Fig. 3(a) which address the essential physics of hybridization of conduction electrons with local moments and the appearance of

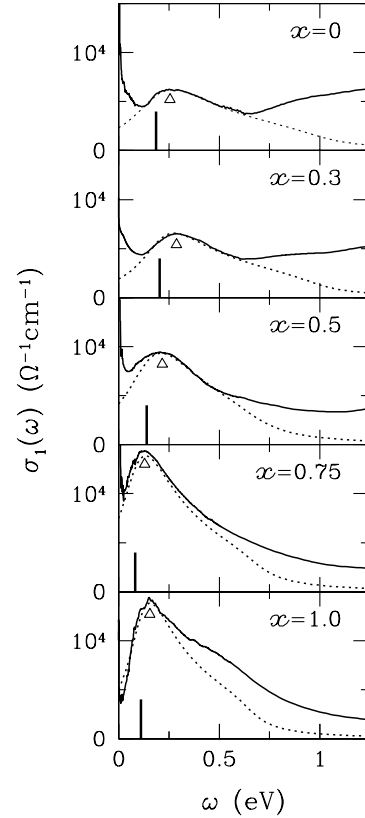


FIG. 1. The real part of the low-temperature optical conductivity of YbIn_{1-x}Ag_xCu₄ ($T = 20$ K) is shown for five values of x . The open triangles mark peak frequencies. The dotted curves refer to a PAM-based joint density-of-states calculation in the text and the dark vertical bars indicate a threshold frequency from that calculation.

the Kondo resonance at E_F . At energies far from the chemical potential, the upper and lower bands, ϵ^+ and ϵ^- , follow closely the unrenormalized free carrier dispersion. Near E_F , the Fermi surface opens (and the bands flatten) to accommodate the f -electron weight projected up to the Fermi level as a result of hybridization. This reorganization of the bands in the vicinity of the Fermi level is due to many-body interactions, the strength of which is characterized by the parameter \tilde{V} . The resultant narrow peak in the density of states, called the Kondo, or Abrikosov-Suhl, resonance is central to the understanding of heavy fermion and mixed-valent phenomenology [15–17].

The hybridization-induced splitting creates the possibility of vertical transitions from filled states below E_F to unoccupied levels above E_F , as illustrated by the arrows of Fig. 3(a). The threshold for these transitions occurs at a frequency $\omega = 2\tilde{V}$, where \tilde{V} is the hybridization strength renormalized by the on-site f -electron repulsion. This energy scales with the Kondo temperature as [11–14,18]

$$\tilde{V} = \sqrt{T_K B}, \quad (2)$$

where B is related to the conduction electron bandwidth [13]. At threshold, the nesting of the coherent (lower) and

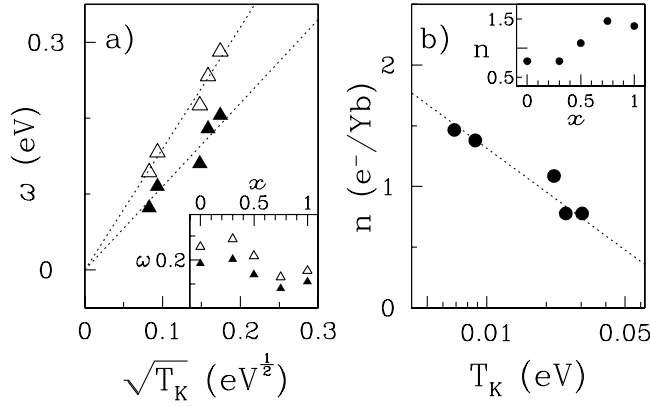


FIG. 2. (a) Characteristic frequencies, ω_{Δ} (Δ) and ω_{th} (\blacktriangle) are shown as a function of x (inset) and the Kondo temperature, T_K . (b) Spectral weight is shown versus x (inset) and T_K . T_K is obtained from low-temperature magnetic susceptibility [1] measurements. Spectral weight is calculated using a bare band mass $m = 4m_e$. Dotted lines show fits to the data based on model equations in the text.

incoherent (upper) bands leads to a very high joint density of states for vertical transitions and hence a strong peak in the conductivity, which we show below can be related with the width of the Kondo resonance, T_K .

To proceed with the analysis, we use the Kubo-Greenwood formula [19]

$$\sigma_1(\omega) = \frac{\pi e^2}{m^2 \omega} \sum_{\ell, \ell'} JDOS_{\ell, \ell'}(\omega) |\mathbf{p}_{\ell, \ell'}|^2, \quad (3)$$

where $|\mathbf{p}_{\ell, \ell'}|$ denotes the dipole matrix element connecting electronic bands ℓ and ℓ' , and $JDOS_{\ell, \ell'}(\omega)$ is the corresponding joint density of states. Applying this formula to hybridizing quasiparticles as though they were electrons allows an exploration of the phenomena of the midinfrared conductivity in the context of the PAM. In that case there are two relevant bands, ϵ^+ and ϵ^- and our model approach leads to

$$\sigma_{\text{pam}}(\omega) = \frac{e^2}{4\pi^2 m^2 \omega} \int_{\Delta=\omega} \frac{dS}{|\nabla_{\mathbf{k}}(\epsilon^+ - \epsilon^-)|} |\mathbf{p}_{+, -}|^2, \quad (4)$$

where $|\mathbf{p}_{+, -}|$ is the matrix element for the one remaining term in the $JDOS_{\ell, \ell'}$ sum of Eq. (3).

For each value of $\omega > 2\tilde{V}$, there are two contributions to the integral: one originating from levels inside the unrenormalized Fermi surface ($k_{<}$); the other from the states occupied as a result of renormalization, i.e., outside the unrenormalized Fermi surface ($k_{>}$). An example of two such transitions with the same ω are indicated by vertical arrows in the inset of Fig. 3.

Simplifying Eq. (4) by making an isotropic approximation and the approximation of a constant $|\mathbf{p}_{+, -}|$ (discussed further below), one obtains

$$\sigma_{\text{pam}}(\omega) = \frac{e^2 |\mathbf{p}_{+, -}|^2}{4\pi^2 m^2 \omega} \sum_{k'=k_{<}, k_{>}} \frac{4\pi k^2}{|\partial_k(\epsilon^+ - \epsilon^-)|} \Big|_{k=k'}. \quad (5)$$

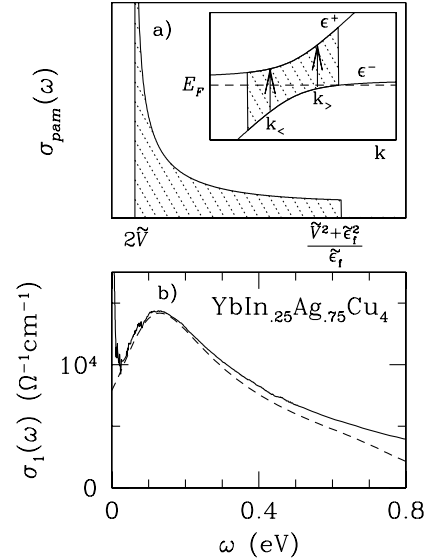


FIG. 3. The inset shows the PAM dispersion relations with arrows indicating transitions made allowed by the existence of the Kondo resonance. (a) shows $\sigma_{\text{pam}}(\omega)$ calculated from those transitions. (b) shows a model conductivity calculated using $\tilde{V} = 41$ meV, $\tilde{\epsilon}_f = 2.5$ meV, $E_F = 1$ eV, $|\mathbf{p}_{+, -}|^2 k_F = 4.673 \text{ \AA}^{-3}$, and $\Delta = 0.12$ eV.

Model spectra can then be calculated using the explicit PAM dispersion relation [16,18],

$$\epsilon^{\pm} = \frac{E_F + \tilde{\epsilon}_f + \epsilon_k \pm \sqrt{(E_F + \tilde{\epsilon}_f - \epsilon_k)^2 + 4\tilde{V}^2}}{2}, \quad (6)$$

where E_F is the Fermi level, \tilde{V} is the renormalized hybridization strength, introduced above, and $\tilde{\epsilon}_f$ is the f -level position renormalized by on-site f -electron repulsion which defines the scale of the low-energy physics and is commonly identified with the impurity Kondo temperature, T_K .

An example of such a calculation for $\tilde{V} = 41$ and $\tilde{\epsilon}_f = 2.5$ meV, is shown in Fig. 3(a). The onset for optical transitions appears as a cusp at $2\tilde{V}$ [20]. While the strength of this cusp is an important feature associated with nesting, the extreme sharpness is an artifact of assuming infinite lifetimes for the quasiparticle states. We rectify this by convoluting this model result with a Lorentzian of constant width to *post hoc* emulate the finite-lifetime effects. The magnitude of the broadening parameter, Δ , gives an estimate of the quasiparticle lifetime. The values used here of around 0.12 eV, correspond to a lifetime of order $\tau = \hbar/\Delta \sim 6$ ps, consistent with pump-probe lifetime measurements of YbAgCu₄ [6].

In Fig. 3(b) we present this calculated $\sigma_{\text{pam}}(\omega)$ together with our measured $\sigma_1(\omega)$ for $x = 0.75$. Based on the quality of this fit, the PAM parameters $\tilde{V} = 41$ and $\tilde{\epsilon}_f = 2.5$ meV can be associated with this composition. With \tilde{V} and $\tilde{\epsilon}_f$ as adjustable parameters, we have similarly modeled the midinfrared conductivity $\sigma_1(\omega)$ for each x value as shown by the dashed curves in Fig. 1. The vertical bars

mark the threshold frequencies $\omega_{th} = 2\tilde{V}$, which are plotted versus x and T_K in Fig. 2(a). The dotted curve through those data shows the consistency between our experimental result and the theoretical scaling of Eq. (2).

With regard to the *total strength*, one can obtain an analytic result in our approach by setting the two sphere areas in (5) equal to $4\pi k_F^2$. This approximation avoids the effects of bare band structure details while including the influence of the strong cusp at $2\tilde{V}$. Solving for the wave vectors $k_>$ and $k_<$ using the condition $\epsilon^+ - \epsilon^- = \omega$, one can obtain a model strength, which is essentially the shaded area of Fig. 3(a), of

$$n_{\text{pam}} = \frac{2m}{\pi e^2} \int_{2\tilde{V}}^{(\tilde{V}^2 + \tilde{\epsilon}_f^2)/\tilde{\epsilon}_f} \sigma_{\text{pam}}(\omega) d\omega \quad (7)$$

$$\simeq \frac{4|\mathbf{p}_{+,-}|^2 k_F}{\pi^2} \ln\left(\frac{\tilde{V}}{\tilde{\epsilon}_f}\right) \quad (8)$$

$$\simeq \frac{4|\mathbf{p}_{+,-}|^2 k_F}{\pi^2} \ln\left(c\sqrt{\frac{B}{T_K}}\right), \quad (9)$$

where c is defined by $T_K = c\tilde{\epsilon}_f$. This logarithmic scaling behavior is compared to the data in Fig. 2(b).

It is important to realize that the simple arguments leading up to Eq. (9) are not strictly rigorous and in fact careful analysis reveals that a \mathbf{k} -independent hybridization leads to a $|\mathbf{p}_{+,-}|$ which depends on \mathbf{k} , and therefore ω , in a manner that will reduce the conductivity at high frequency [12]. One expects that in a real system, transitions between Cu-In-Ag d orbital bands and Yb f -band states are likely to be allowed due to their relative spatial displacement. Incorporation of this possibility into theory can be done by allowing a dispersive $\tilde{V}_{\mathbf{k}}$, which would tend to restore some of the high-frequency conductivity that is underestimated in our simplified approach. A more sophisticated approach to $n(T_K)$ would be valuable in the ongoing effort toward a quantitative understanding of strongly correlated electrodynamics.

Equations (2) and (9) qualitatively explain the observed dependence of the frequency and strength on T_K . In addition these equations show an interesting relationship between the scaling of $n(T_K)$ and $\omega_{th}(T_K)$. Using the impurity model result for c [21], and fitting the measured $n(T_K)$ to Eq. (9), one gets a value for the band parameter $B = 0.36$ eV. This value is determined solely by the extrapolation of the data to the T_K axis, and so does not depend on k_F or the matrix elements present in the coefficient of the logarithm. One can independently obtain a value for B from fitting the T_K dependence of the excitation frequency [Fig. 2(a)], $\omega_{th} = 2\tilde{V} = 2\sqrt{T_K B}$, which leads to $B = 0.30$ eV. The observation that these independently obtained values of B are comparable shows a nontrivial relationship between the scaling behavior of strength and characteristic frequency in our optical data. These results indicate that T_K scaling is present in the

low-temperature dynamics of $\text{YbIn}_{1-x}\text{Ag}_x\text{Cu}_4$ and can be addressed in the context of local-moment models. Further work may be directed toward greater understanding of this low- T scaling behavior as well as unexplained temperature dependent behavior of $\text{YbIn}_{1-x}\text{Ag}_x\text{Cu}_4$.

The authors acknowledge extremely valuable discussions with D. L. Cox as well as D. N. Basov, A. L. Cornelius, P. A. Lee, B. S. Shastry, and A. P. Young. We also gratefully acknowledge assistance from S. L. Hoobler and Y. W. Rodriguez. This work is supported by NSF DMR-0071949 and DMR-0203214.

-
- [1] A. L. Cornelius, J. M. Lawrence, J. L. Sarrao, Z. Fisk, M. F. Hundley, G. H. Kwei, J. D. Thompson, C. H. Booth, and F. Bridges, *Phys. Rev. B* **56**, 7993 (1997).
 - [2] J. Sarrao, C. Immer, C. Benton, Z. Fisk, J. Lawrence, D. Mandrus, and J. Thompson, *Phys. Rev. B* **54**, 12 207 (1996).
 - [3] B. Kindler, R. Graf, F. Ritter, W. Assmus, and B. Luthi, *Phys. Rev. B* **50**, 704 (1994).
 - [4] J. Lawrence, G. Kwei, J. Sarrao, Z. Fisk, D. Mandrus, and J. Thompson, *Phys. Rev. B* **54**, 6011 (1996).
 - [5] S. L. Garner, J. N. Hancock, Y. W. Rodriguez, Z. Schlesinger, B. Bucher, J. L. Sarrao, and Z. Fisk, *Phys. Rev. B* **62**, R4778 (2000).
 - [6] J. Demsar, R. D. Averitt, K. H. Ahn, M. J. Graf, S. A. Trugman, V. V. Kabanov, J. L. Sarrao, and A. J. Taylor, *Phys. Rev. Lett.* **91**, 027401 (2003).
 - [7] J. Freericks and V. Zlatic, *Phys. Rev. B* **58**, 322 (1998).
 - [8] T. Giamarchi, C. M. Varma, A. E. Ruckenstein, and P. Nozières, *Phys. Rev. Lett.* **70**, 3967 (1993).
 - [9] S. V. Dordevic, D. N. Basov, N. R. Dilley, E. D. Bauer, and M. B. Maple, *Phys. Rev. Lett.* **86**, 684 (2001).
 - [10] L. Degiorgi, F. Anders, and G. Gruner, *Eur. Phys. J. B* **19**, 167 (2001).
 - [11] P. Coleman, *Phys. Rev. Lett.* **59**, 1026 (1987).
 - [12] D. L. Cox (personal communication).
 - [13] A. J. Millis and P. A. Lee, *Phys. Rev. B* **35**, 3394 (1987).
 - [14] A. J. Millis, M. Lavagna, and P. A. Lee, *Phys. Rev. B* **36**, 864 (1987).
 - [15] L. Degiorgi, *Rev. Mod. Phys.* **71**, 687 (1999).
 - [16] A. Hewson, *The Kondo Problem to Heavy Fermions* (Cambridge University Press, New York, 1993).
 - [17] M. Jarrell, *Phys. Rev. B* **51**, 7429 (1995).
 - [18] N. Grewe, *Z. Phys. B* **56**, 111 (1984).
 - [19] M. Dressel and G. Gruner, *Electrodynamics of Solids: Optical Properties of Electrons in Matter* (Cambridge University Press, New York, 2002).
 - [20] A second feature of the theoretical $\sigma_{\text{pam}}(\omega)$ occurs at a higher frequency $\omega = (\tilde{V}^2 + \tilde{\epsilon}_f^2)/\tilde{\epsilon}_f$, and results from the initial state energy exceeding E_F , where no occupied levels are available. This high energy scale is of order the bandwidth and is used as the upper limit of integration.
 - [21] For $N = 2j + 1 = 8$, the Fermi liquid theory of the Anderson impurity model predicts [16] $\tilde{\epsilon}_f = k_B T_K N^2 2 \sin(2\pi/N)/w_N \pi(N-1) \simeq 1.517 T_K$.